FULL PAPER

Dalton
www.rsc.org/dalton

Synthesis, structures and properties of a series of novel left- and right-handed metal coordination double helicates with chiral channels

Chuan-De Wu, Can-Zhong Lu,* Shao-Fang Lu, Hong-Hui Zhuang and Jin-Shun Huang
The State Key Laboratory of Structural Chemistry, Fujian Institute of Research on the Structure of Matter, the Chinese Academy of Sciences, Fuzhou, Fujian, 350002, P.R. China

Received 8th April 2003, Accepted 24th June 2003
First published as an Advance Article on the web 14th July 2003

The reactions of $LnCl_3$ (Ln = lanthanide cations), L- or D-tartaric acid and molybdate in acidified aqueous solutions gave rise to the enantiopure left- or right-handed double helical coordination metal compounds, $\{A[Mo_2^{VI}O_4Ln^{III}(H_2O)_6(C_4H_2O_6)_2]\cdot 4H_2O\}_n$ (Ln = Sm, Eu, Gd, Ho, Yb, Y; $C_4H_2O_6$ = L- or D-tartaric acid; A = NH_4 or H_3O; **MoLn** represent all complexes), which have been characterized by single X-ray crystal structure analyses, IR, FT-Raman, TGA, XRPD, electric conductivity, EPR and magnetic susceptibility studies. The TGA and XRPD studies for compound **MoGd** suggest that the backbone is "collapsed" with the removement of aqua ligands and crystallization water molecules. However, it is easily reverted to the original compound after being immersed in water, as confirmed by similar XRPD patterns. The electric conductivity studies for these compounds reveal they are semiconductors. As aforementioned, the conductivity behaviors for the dry sample and reversed sample of **MoGd** are also very similar, in line with the XPRD results. Study of the magnetic susceptibilities reveal that the magnetic behaviors for **MoGd**, **MoDy**, **MoHo** and **MoYb** obey the Curie–Weiss law.

Introduction

In recent years, chemists have devoted a great deal of effort to assemble biomimetic materials by linking up simple building blocks. The studies on the construction of artificial systems stem from their potential applications, such as, medicine, electrical conductivity, magnetism, molecular selection, ion exchange, catalysis and enantioselectivity, as well as the intriguing varieties of architectures and topologies.[1–11]

The formation of helical, especially double helical structures, by assembly of metal coordination species has received a great deal of attention. This is not only because of their intriguing structures, but also their potential applications in many fields, such as, asymmetric catalysis, optical devices, *etc*. Most strategies for designing such chiral coordination polymeric architectures are, in principle, generated by self-assembly of chiral building blocks, which usually involve the use of chiral ligands and/or chiral metal coordination fragments. Many chemists have been making great contributions to this field, and recently quite a few significant papers concerning helical or double helical compounds have been reported.[10–16] Among the vast majority of reported work, the synthesis of organic–inorganic compounds containing double-helical arrays is of particular interest. A system based on chiral organic ligands linking up tetrahedrally coordinated Ag^+, Cu^+ or binary coordinated Ag^+ ions (acting as "chiral metal centers") in the ratio of 2 : 1 has been widely studied, where such coordination of central metal ions often spontaneously generate compounds with double helical geometry.[13] Another important system is of inorganic double helical cores, which is generated from the combination of vanadium phosphate[14] or tetracoordinated copper(I) atoms[15] or $\{Cu^{II}O_4N\}$ square pyramids linked by $\{Mo^{VI}O_4\}$ tetrahedra.[16] These materials have set up a stage for the development of helical structures. During our investigations on chiral architecture compounds, we have set up a strategy for the design of chiral self-assembly systems, especially those derived from chiral ligands coordinated to metal fragments, which act as connecting units or templates. For example, the chiral carboxylic acid ligands bridged to highly oxophilic molybdenum and lanthanide atoms can be used to induce diastereoselectivity in the formation of the helical structures. Most interestingly, we have found that L-tartaric acid is capable of coordinating to molybdenum and lanthanide atoms to lead to the formation of novel coordination left-handed double helicates.[17] As an extension of our previous work, we now report herein the syntheses, crystal structures, and some physical properties studies of a series of novel L- or D-tartaric acid coordinating enantiopure coordination compounds with left- or right-handed double helical chain arrays, $\{A[Mo_2^{VI}O_4Ln^{III}(H_2O)_6(C_4H_2O_6)_2]\cdot 4H_2O\}_n$ (Ln = Sm, Eu, Gd, Ho, Yb, Y; $C_4H_2O_6$ = L- or D-tartaric acid; A = NH_4 or H_3O; **MoLn** represent all complexes).

Experimental

Materials

All chemicals were of reagent grade and were used as received. Elemental analyses were performed with a Vario EL III CHNOS Element Analyzer. Infrared spectra were recorded on a FTS-40 spectrophotometer by use of pressed KBr pellets. The FT-Raman spectra were measured on a Nicolet Raman 910 Flourier transform laser-Raman spectrum by use of pressed KBr pellets and EPR was performed on a Bruker ER 420 model. Variable temperature magnetic susceptibilities were measured on a model CF-1 superconducting extracting sample magnetometer with the powder sample kept in a capsule for weighing. All data were corrected for diamagnetism of the ligands estimated from Pascal's constants.[18] Electrical conductivity data were measured on a ZL5-SMART-LCR instrument. Thermogravimetric analyses (TGA), using a universal V2.4F TA Instrument, were performed on powder samples of compounds **MoLn** in flowing N_2 with a heating rate of 10 °C min^{-1} in the temperature range 30–800 °C.

Synthesis

$\{NH_4[Mo_2^{VI}O_4Sm^{III}(H_2O)_6(L\text{-}C_4H_2O_6)_2]\cdot 4H_2O\}_n$ (MoSm). Sm_2O_3 (0.87 g, 2.5 mmol) was dissolved in 10 mL concentrated HCl under heating for about 5 min, the resulting solution was added to an acidified solution of $(NH_4)_6Mo_7O_{24}\cdot 4H_2O$ (1.8 g, 1.46 mmol in 120 ml water) in the presence of L-tartaric acid (1.50 g, 10 mmol), the solution was then adjusted to pH = 0.80 by 10% HCl. Colorless crystals of **MoSm** were isolated in high yield after one week (4.3 g, 97.9%). Anal. Calc. for **MoSm** (%): C 10.72, H 3.15, N 1.56. Found: C 10.66, H 3.13, N 1.61. The

DOI: 10.1039/b303943a

This journal is © The Royal Society of Chemistry 2003

Table 1 Crystal data and structure refinement for **MoLn** (Ln = Sm, Eu, Gd, Ho, Yb, Y)

	MoSm	K–MoSm	D-MoSm	MoEu
Formula	$C_8H_{28}NO_{26}Mo_2Sm$	$C_8H_{27}O_{27}Mo_2Sm$	$C_8H_{28}NO_{26}Mo_2Sm$	$C_8H_{28}NO_{26}Mo_2Eu$
Formula weight	896.54	897.53	896.54	898.15
Crystal color	Colorless	Colorless	Colorless	Colorless
Crystal system	Hexagonal	Hexagonal	Hexagonal	Hexagonal
Space group	$P6_522$	$P6_522$	$P6_122$	$P6_522$
Unit cell dimensions/Å	a = 15.339(1)	a = 15.374(1)	a = 15.329(1)	a = 15.335(1)
	c = 18.668(4)	c = 18.741(1)	c = 18.707(1)	c = 18.744(1)
V/Å^3	3803.9(9)	3836.0(1)	3806.5(1)	3817.3(1)
Z	6	6	6	6
D_c/g cm^{-3}	2.348	2.331	2.347	2.344
F(000)	2622	2622	2622	2628
μ/mm^{-1}	3.371	3.345	3.369	3.517
Reflections collected	14903	9952	19376	9320
Unique reflections /parameters	2253/184	2258/183	2240/185	2253/181
Goodness-of-fit on F^2	1.117	1.076	1.095	1.073
Flack parameters	−0.003(17)	−0.01(3)	−0.015(16)	0.00(3)
$R1$ ($wR2$) ($I > 2\sigma(I)$)	0.0294 (0.0656)	0.0434 (0.0859)	0.0265 (0.0654)	0.0451 (0.0850)
$R1$ ($wR2$) (all data)	0.0384 (0.0699)	0.0702 (0.0969)	0.0287 (0.0675)	0.0780 (0.0949)
Largest diff. peak, hole/e Å^{-3}	0.467, −0.467	0.731, −0.580	0.623, −0.402	0.803, −0.784

	MoGd	MoHo	MoYb	MoY
Formula	$C_8H_{28}NO_{26}Mo_2Gd$	$C_8H_{28}NO_{26}Mo_2Ho$	$C_8H_{28}NO_{26}Mo_2Yb$	$C_8H_{28}NO_{26}Mo_2Y$
Formula weight	903.44	911.12	919.23	835.10
Crystal color	Colorless	Pink	Colorless	Colorless
Crystal system	Hexagonal	Hexagonal	Hexagonal	Hexagonal
Space group	$P6_522$	$P6_522$	$P6_522$	$P6_522$
Unit cell dimensions/Å	a = 15.298(1)	a = 15.302(1)	a = 15.265(1)	a = 15.295(1)
	c = 18.661(1)	c = 18.550(1)	c = 18.475(1)	c = 18.597(2)
V/Å^3	3782.2(1)	3761.5(1)	3728.0(1)	3767.8(6)
Z	6	6	6	6
D_c/g cm^{-3}	2.380	2.413	2.457	2.208
F(000)	2634	2652	2670	2484
μ/mm^{-1}	3.692	4.223	4.840	3.388
Reflections collected	11491	11541	12074	8448
Unique reflections/parameters	2252/184	1735/183	2194/176	2237/173
Goodness-of-fit on F^2	1.088	1.055	1.112	1.023
Flack parameters	−0.003(14)	−0.01(3)	0.011(16)	−0.03(3)
$R1$($wR2$) ($I > 2\sigma(I)$)	0.0258 (0.0607)	0.0509 (0.0911)	0.0391 (0.0787)	0.0683 (0.1226)
$R1$($wR2$) (all data)	0.0333 (0.0639)	0.0809 (0.1000)	0.0527 (0.0836)	0.1583 (0.1547)
Largest diff. peak, hole/e Å^{-3}	0.540, −0.424	0.627, −0.435	0.712, −0.665	0.841, −0.678

$R1 = \Sigma(|F_o| - |F_c|)/\Sigma|F_o|$, $wR2 = [\Sigma w(F_o^2 - F_c^2)^2/\Sigma w(F_o^2)^2]^{0.5}$.

IR spectrum of **MoSm** exhibits broad bands at 1630–1068 cm^{-1}, which can be assigned to ligand vibrations, and at 928–501 cm^{-1} to the ν(Mo=O) or ν(Mo–O) bending vibrations. Similarly, the Raman data at 1594–1060 cm^{-1} is for the ligands and at 942–169 cm^{-1} for ν(Mo=O) or ν(Mo–O–Mo), respectively.

$\{[NH_4][Mo_2^{VI}O_4Ln^{III}(H_2O)_6(L\text{-}C_4H_2O_6)_2]\cdot 4H_2O\}_n$ [Ln = Eu (MoEu), Gd (MoGd), Ho (MoHo), Yb (MoYb), Y (MoY)]. These compounds were obtained following the method as described above for the compound **MoSm**, except using Ln_2O_3 (Ln = Eu, Gd, Ho, Yb, Y) instead of Sm_2O_3. The yields all exceeded 90%. Anal. Calc. for **MoEu** (%): C, 10.70, H, 3.14, N, 1.56. Found: C, 10.67, H, 3.19, N, 1.50. Anal. Calc. for **MoGd** (%): C 10.64, H 3.12, N 1.55. Found: C 10.71, H 3.16, N 1.61. Anal. Calc. for **MoYb** (%): C 10.45, H 3.07, N 1.52. Found: C 10.45, H 3.05, N 1.50. Anal. Calc. for **MoY** (%): C 11.51, H 3.38, N 1.68. Found: C 11.46, H 3.38, N 1.69.

$\{[NH_4][Mo_2^{VI}O_4Sm^{III}(H_2O)_6(L\text{-}C_4H_2O_6)_2]\cdot 4H_2O\}_n$ (D-MoSm). The synthesis of this compound was as above for the compound **MoSm**, except that D-tartaric acid was used instead of L-tartaric acid.

$\{[H_3O][Mo_2^{VI}O_4Sm^{III}(H_2O)_6(L\text{-}C_4H_2O_6)_2]\cdot 4H_2O\}_n$ (K–MoSm). The synthesis of this compound was as above for the compound **MoSm**, except that potassium molybdate was used instead of ammonium molybdate.

Crystal structure determination

The determinations of the unit cells and the data collections for the prismatic crystals of compounds **MoLn** were performed on a Siemens SMART CCD, and the data were collected using graphite-monochromated Mo-Kα radiation (λ = 0.71073 Å) at 293 K. The data sets were corrected by the SADABS program.[19] The structures were solved by direct methods, and were refined by full-matrix least-squares method with the SHELXL-97[20] program package. The hydrogen atoms on carbon atoms were positioned geometrically, while the hydrogen atoms of ammonium and water were not located. Crystallographic data for compounds **MoLn** are summarized in Table 1, selected bond lengths and angles are listed in Tables 2 and 3, with selected hydrogen bond distances in Table 4.

CCDC reference numbers 175443 (**MoSm**), 175444 (D-MoSm), 208057 (**K–MoSm**), 208058 (**MoEu**), 203714 (**MoGd**), 208059 (**MoHo**), 200621 (**MoYb**) and 208060 (**MoY**).

See http://www.rsc.org/suppdata/dt/b3/b303943a/ for crystallographic data in CIF or other electronic format.

Results and discussion

Synthesis

MoLn were simply synthesized from following methods: Ln_2O_3 were dissolved in concentrated HCl under heating, the resulting solutions were added to an acidified solution of molybdate in

Table 2 Selected bond lengths (Å) for compounds **MoLn** (Ln = Sm, Eu, Gd, Ho, Yb, Y)

MoSm		K–MoSm		D-MoSm		MoEu	
Sm–O(2)	2.367(4)	Sm–O(2)	2.374(7)	Sm–O(7)	2.371(4)	Eu–O(2)	2.366(7)
Sm–O(9)	2.417(6)	Sm–O(9)	2.404(9)	Sm–O(1)	2.407(5)	Eu–O(10)	2.410(8)
Sm–O(10)	2.433(6)	Sm–O(10)	2.425(8)	Sm–O(3)	2.428(5)	Eu–O(9)	2.412(8)
Sm–O(11)	2.473(5)	Sm–O(11)	2.483(8)	Sm–O(2)	2.475(5)	Eu–O(11)	2.461(7)
Mo–O(8)	1.701(4)	Mo–O(8)	1.684(7)	Mo–O(6)	1.706(4)	Mo–O(8)	1.691(7)
Mo–O(7)	1.708(4)	Mo–O(7)	1.710(7)	Mo–O(4)	1.719(4)	Mo–O(7)	1.710(7)
Mo–O(3)	1.944(5)	Mo–O(3)	1.953(7)	Mo–O(11)	1.950(4)	Mo–O(4)^{i}	1.942(8)
Mo–O(4)^{i}	1.946(5)	Mo–O(4)^{i}	1.959(7)	Mo–O(9)	1.959(4)	Mo–O(3)	1.950(7)
Mo–O(6)^{i}	2.209(5)	Mo–O(6)^{i}	2.221(7)	Mo–O(10)	2.221(4)	Mo–O(6)^{i}	2.203(7)
Mo–O(1)	2.229(4)	Mo–O(1)	2.237(7)	Mo–O(5)	2.234(4)	Mo–O(1)	2.233(7)
MoGd		**MoHo**		**MoYb**		**MoY**	
Gd–O(2)	2.348(4)	Ho–O(2)	2.309(9)	Yb–O(2)	2.265(6)	Y–O(2)	2.307(10)
Gd–O(9)	2.387(5)	Ho–O(9)	2.368(11)	Yb–O(9)	2.315(8)	Y–O(9)	2.349(10)
Gd–O(10)	2.388(5)	Ho–O(10)	2.375(12)	Yb–O(10)	2.339(8)	Y–O(10)	2.387(11)
Gd–O(11)	2.442(5)	Ho–O(11)	2.436(10)	Yb–O(11)	2.394(7)	Y–O(11)	2.405(10)
Mo–O(8)	1.698(4)	Mo–O(8)	1.700(10)	Mo–O(7)	1.705(6)	Mo–O(8)	1.707(10)
Mo–O(7)	1.702(4)	Mo–O(7)	1.706(10)	Mo–O(8)	1.711(7)	Mo–O(7)	1.712(10)
Mo–O(4)^{i}	1.942(4)	Mo–O(4)^{i}	1.959(11)	Mo–O(3)	1.941(7)	Mo–O(4)^{i}	1.952(10)
Mo–O(3)	1.947(4)	Mo–O(3)	1.968(10)	Mo–O(4)^{i}	1.946(7)	Mo–O(3)	1.952(11)
Mo–O(6)^{i}	2.203(4)	Mo–O(6)^{i}	2.213(11)	Mo–O(6)^{i}	2.201(6)	Mo–O(6)^{i}	2.199(11)
Mo–O(1)	2.224(4)	Mo–O(1)	2.244(9)	Mo–O(1)	2.241(6)	Mo–O(1)	2.235(10)

Table 3 Selected bond angles (°) for compounds **MoLn** (Ln = Sm, Eu, Gd, Ho, Yb, Y)

MoSm		K–MoSm		D-MoSm		MoEu	
O(2)^{ii}–Sm–O(2)	148.3(2)	O(2)^{ii}–Sm–O(2)	148.0(4)	O(7)^{iii}–Sm–O(7)	148.3(2)	O(2)^{ii}–Eu–O(2)	148.6(4)
O(2)–Sm–O(9)	89.21(2)	O(2)–Sm–O(9)	89.8(3)	O(7)^{iii}–Sm–O(1)	100.7(2)	O(2)–Eu–O(10)	74.1(3)
O(2)–Sm–O(9)^{ii}	101.4(2)	O(2)–Sm–O(9)^{ii}	100.9(3)	O(7)–Sm–O(1)	90.0(2)	O(2)–Eu–O(10)^{ii}	81.0(3)
O(9)–Sm–O(9)^{ii}	140.8(4)	O(9)–Sm–O(9)^{ii}	140.5(6)	O(1)–Sm–O(1)^{iii}	140.1(4)	O(10)–Eu–O(10)^{ii}	74.8(6)
O(2)–Sm–O(10)^{ii}	81.4(2)	O(2)–Sm–O(10)	73.8(3)	O(7)–Sm–O(3)	74.1(2)	O(2)–Eu–O(9)	88.7(3)
O(9)–Sm–O(10)^{ii}	146.6(3)	O(9)–Sm–O(10)	72.5(4)	O(1)–Sm–O(3)	73.0(3)	O(10)–Eu–O(9)	72.3(4)
O(2)–Sm–O(10)	73.3(2)	O(2)–Sm–O(10)^{ii}	80.8(3)	O(7)–Sm–O(3)^{iii}	80.7(2)	O(2)–Eu–O(9)^{ii}	101.8(3)
O(9)–Sm–O(10)	72.6(3)	O(9)–Sm–O(10^{ii}	147.0(4)	O(1)–Sm–O(3)^{iii}	146.9(3)	O(10)–Eu–O(9)^{ii}	147.1(4)
O(10)^{ii}–Sm–O(10)	74.0(4)	O(10)–Sm–O(10)^{ii}	74.5(6)	O(3)–Sm–O(3)^{iii}	73.9(4)	O(9)–Eu–O(9)^{ii}	140.6(5)
O(2)–Sm–O(11)^{ii}	142.4(2)	O(2)–Sm–O(11)^{ii}	142.6(3)	O(7)–Sm–O(2)^{iii}	142.5(2)	O(2)–Eu–O(11)^{ii}	142.1(3)
O(9)–Sm–O(11)^{ii}	73.9(2)	O(9)–Sm–O(11)^{ii}	73.4(3)	O(1)–Sm–O(2)^{iii}	73.5(2)	O(10)–Eu–O(11)^{ii}	128.2(3)
O(10)–Sm–O(11)^{ii}	129.2(3)	O(10)–Sm–O(11)^{ii}	128.6(4)	O(3)–Sm–O(2)^{iii}	128.9(3)	O(9)–Eu–O(11)^{ii}	73.7(3)
O(2)–Sm–O(11)	69.2(2)	O(2)–Sm–O(11)	69.3(3)	O(7)–Sm–O(2)	69.1(2)	O(2)–Eu–O(11)	69.1(3)
O(9)–Sm–O(11)	75.0(2)	O(9)–Sm–O(11)	75.3(4)	O(1)–Sm–O(2)	74.9(3)	O(10)–Eu–O(11)	130.6(3)
O(10)–Sm–O(11)	130.0(2)	O(10)–Sm–O(11)	130.3(3)	O(3)–Sm–O(2)	130.3(2)	O(9)–Eu–O(11)	75.1(3)
O(11)^{ii}–Sm–O(11)	74.0(3)	O(11)^{ii}–Sm–O(11)	74.1(4)	O(2)^{iii}–Sm–O(2)	74.1(3)	O(11)^{ii}–Eu–O(11)	74.0(4)
MoGd		**MoHo**		**MoYb**		**MoY**	
O(2^{ii}–Gd–O(2)	148.2(2)	O(2)^{ii}–Ho–O(2)	147.5(5)	O(2)^{ii}–Yb–O(2)	148.2(3)	O(2)^{ii}–Y–O(2)	149.1(5)
O(2)–Gd–O(9)	88.7(2)	O(2)–Ho–O(9)	88.5(4)	O(2)–Yb–O(9)	88.9(3)	O(2)–Y–O(9)	89.6(4)
O(2)–Gd–O(9)^{ii}	101.9(2)	O(2)–Ho–O(9)^{ii}	102.1(3)	O(2)–Yb–O(9)^{ii}	101.5(2)	O(2)–Y–O(9)^{ii}	100.7(4)
O(9)–Gd–O(9)^{ii}	141.1(3)	O(9)–Ho–O(9)^{ii}	142.0(7)	O(9)–Yb–O(9)^{ii}	141.4(5)	O(9)–Y–O(9)^{ii}	140.9(7)
O(2)–Gd–O(10)	73.6(2)	O(2)–Ho–O(10)	72.9(4)	O(2)–Yb–O(10)	73.9(3)	O(2)–Y–O(10)	74.1(4)
O(9)–Gd–O(10)	72.4(3)	O(9)–Ho–O(10)	71.8(6)	O(9)–Yb–O(10)	72.3(4)	O(9)–Y–O(10)	72.1(5)
O(2)–Gd–O(10)^{ii}	81.1(2)	O(2)–Ho–O(10)^{ii}	81.3(4)	O(2)–Yb–O(10)^{ii}	80.8(3)	O(2)–Y–O(10)^{ii}	81.4(4)
O(9)–Gd–O(10)^{ii}	146.5(2)	O(9)–Ho–O(10)^{ii}	146.2(5)	O(9)–Yb–O(10)^{ii}	146.3(4)	O(9)–Y–O(10)^{ii}	147.0(5)
O(10)–Gd–O(10)^{ii}	74.1(4)	O(10)–Ho–O(10)^{ii}	74.5(9)	O(10)–Yb–O(10)^{ii}	74.0(6)	O(10)–Y–O(10)^{ii}	75.0(7)
O(2)–Gd–O(11)^{ii}	142.4(2)	O(2)–Ho–O(11)^{ii}	143.0(3)	O(2)–Yb–O(11)^{ii}	142.2(3)	O(2)–Y–O(11)^{ii}	142.1(4)
O(9)–Gd–O(11)^{ii}	74.3(2)	O(9)–Ho–O(11)^{ii}	74.7(4)	O(9)–Yb–O(11)^{ii}	74.6(3)	O(9)–Y–O(11)^{ii}	73.9(4)
O(10)–Gd–O(11)^{ii}	128.9(2)	O(10)–Ho–O(11)^{ii}	128.9(5)	O(10)–Yb–O(11)^{ii}	129.2(3)	O(10)–Y–O(11)^{ii}	128.8(4)
O(2)–Gd–O(11)	69.2(2)	O(2)–Ho–O(11)	69.3(4)	O(2)–Yb–O(11)	69.4(3)	O(2)–Y–O(11)	68.7(4)
O(9)–Gd–O(11)	74.9(2)	O(9)–Ho–O(11)	75.3(5)	O(9)–Yb–O(11)	74.7(3)	O(9)–Y–O(11)	75.1(4)
O(10)–Gd–O(11)	130.3(2)	O(10)–Ho–O(11)	129.7(4)	O(10)–Yb–O(11)	130.4(3)	O(10)–Y–O(11)	129.8(4)
O(11)^{ii}–Gd–O(11)	74.0(3)	O(11)^{ii}–Ho–O(11)	74.6(5)	O(11)^{ii}–Yb–O(11)	73.5(4)	O(11)^{ii}–Y–O(11)	74.1(5)

Symmetry transformations used to generate equivalent atoms: i): $y + 1, -x + y + 1, z + 1/6$; ii): $-y + 1, -x + 1, -z + 1/6$; iii): $x, x - y, -z + 1/6$.

the presence of L- or D-tartaric acid at low pH values. It is striking that the isolated compounds are composed of left- or right-handed double helices, which are constructed from very simple basic building blocks linked by L- or D-tartaric acid. Detailed experiments suggest that the pH values of the reaction solutions within the 0.3–3.0 range are the best acidic conditions for the formation for compounds **MoLn**. However, the best pH values for the formation of crystals suitable for single X-ray studies are in the 0.3–1.5 range. We have tried using potassium molybdate instead of ammonium molybdate to determine the possible positions of cations. Unfortunately, only protonated water molecules were found as cations. This result suggests that there are no suitable voids for the accommodation of potassium cations, which might be accounted for

Table 4 Selected hydrogen bond lengths (Å) for **MoLn** (Ln = Sm, Eu, Gd, Ho, Yb, Y)

MoSm		K–MoSm		D-MoSm		MoEu	
D ⋯ A	*d*(D ⋯ A)	D ⋯ A	*d*(D ⋯ A)	D ⋯ A	*d*(D ⋯ A)	D ⋯ A	*d*(D ⋯ A)
O(3)–O(104)	2.97(2)	O(3)–O(104)	2.87(2)	O(101)–O(6)	2.88(1)	O(3)–O(104)	2.83(2)
O(7)–N(1)	2.78(1)	O(7)–O(105)	2.79(1)	O(101)–O(104)[g]	2.89(2)	O(7)–N(1)	2.75(1)
O(8)–O(103)	2.70(1)	O(8)–O(103)	2.75(2)	O(101)–O(105)[g]	2.96(2)	O(8)–O(103)	2.77(3)
O(8)–O(102)	2.93(1)	O(8)–O(102)	2.90(1)	O(102)–O(103)[h]	2.98(2)	O(8)–O(102)	3.01(2)
O(9)–O(6)[a]	2.93(1)	O(9)–O(6)[a]	2.94(1)	O(102)–O(1)[i]	2.98(2)	O(9)–O(6)[a]	2.91(1)
O(11)–O(5)[b]	2.71(1)	O(11)–O(5)[b]	2.72(1)	O(102)–O(5)[j]	2.96(1)	O(11)–O(5)[b]	2.70(1)
O(101)–O(9)[c]	2.74(1)	O(101)–O(9)[c]	2.78(2)	O(103)–O(11)	2.87(1)	O(101)–O(9)[c]	2.78(1)
O(101)–O(104)[d]	2.83(2)	O(101)–O(1)[e]	2.92(1)	O(104)–O(4)[h]	2.94(2)	O(101)–O(1)[e]	2.93(2)
O(101)–O(1)[e]	2.97(1)	O(101)–O(104)[d]	3.07(3)	O(1)–O(10)[k]	2.92(1)	O(101)–O(104)[d]	3.12(3)
O(103)–O(7)[d]	2.89(1)	O(103)–O(7)[d]	3.06(2)	O(2)–O(7)	2.75(1)	O(103)–O(7)[d]	2.80(3)
O(104)–O(9)[f]	2.87(2)	O(104)–O(9)[f]	3.09(2)	O(2)–O(8)[l]	2.94(2)	O(104)–O(9)[f]	3.17(2)
N(1)–O(10)[d]	2.71(1)	O(105)–O(10)[d]	2.73(1)	O(3)–O(7)	2.89(1)	N(1)–O(10)[d]	2.72(1)

MoGd		MoHo		MoYb		MoY	
D ⋯ A	*d*(D ⋯ A)	D ⋯ A	*d*(D ⋯ A)	D ⋯ A	*d*(D ⋯ A)	D ⋯ A	*d*(D ⋯ A)
O(3)–O(104)	2.85(1)	O(3)–O(104)	2.94(3)	O(3)–O(104)	2.93(2)	O(3)–O(104)	2.81(3)
O(7)–N(1)	2.77(1)	O(7)–N(1)	2.77(1)	O(7)–N(1)	2.76(1)	O(7)–N(1)	2.77(1)
O(8)–O(103)	2.72(1)	O(8)–O(103)	2.75(2)	O(8)–O(103)	2.71(1)	O(8)–O(103)	2.68(2)
O(8)–O(102)	2.95(1)	O(8)–O(102)	2.90(2)	O(8)–O(102)	2.88(1)	O(8)–O(102)	2.94(2)
O(9)–O(6)[a]	2.93(1)	O(9)–O(6)[a]	2.94(2)	O(9)–O(6)[a]	2.96(1)	O(9)–O(6)[a]	2.94(2)
O(11)–O(5)[b]	2.71(1)	O(11)–O(5)[b]	2.74(2)	O(11)–O(5)[b]	2.74(1)	O(11)–O(5)[b]	2.75(2)
O(101)–O(9)[c]	2.78(1)	O(101)–O(9)[c]	2.74(2)	O(101)–O(9)[c]	2.75(2)	O(101)–O(9)[c]	2.72(2)
O(101)–O(1)[e]	2.91(1)	O(101)–O(104)[d]	2.87(5)	O(101)–O(104)[d]	2.88(3)	O(101)–O(1)[e]	2.97(2)
O(101)–O(104)[d]	3.01(2)	O(101)–O(1)[e]	2.90(2)	O(101)–O(1)[e]	2.91(2)	O(101)–O(104)[d]	2.98(4)
O(103)–O(7)[d]	2.87(1)	O(103)–O(7)[d]	2.86(3)	O(103)–O(7)[d]	2.89(2)	O(103)–O(7)[d]	2.94(3)
O(104)–O(9)[f]	3.07(2)	O(104)–O(9)[f]	2.93(3)	O(104)–O(9)[f]	2.96(2)	O(104)–O(9)[f]	3.12(3)
N(1)–O(10)[d]	2.71(1)	N(1)–O(10)[d]	2.73(2)	N(1)–O(10)[d]	2.72(1)	N(1)–O(10)[d]	2.72(2)

Symmetry transformations used to generate equivalent atoms: a): $-x+1, -x+y+1, -z+1/3$; b): $x-y, x, z-1/6$; c): $-y+1, x-y, z+2/3$; d): $y+1, -x+y+1, z+1/6$; e): $x, x-y, -z+5/6$; f): $-x+1, -y, z+1/2$; g): $x-y, x, -z+1$; h): $x-y, x, z+1/6$; i): $-x+y+1, -x+1, z+2/3$; j): $-y+1, -x+1, -z+5/6$; k): $-x+y+1, y, -z+1/2$; l): $-x+y+1, -x+1, z-1/3$.

by the slightly different cation sizes between NH_4^+ and K^+ cations.

Description of crystal structures

The structural analyses reveal that **MoLn** are left- or right-handed double helicates. The crystal data show these compounds are isostructural, the unit cell dimensions, volumes, related bond distances and angles are only slightly changed as a consequence of lanthanide shrinking. A representative structure of the symmetry expanded structures and the coordination environments around Mo and Ln atoms in **MoLn** is shown in Fig. 1 (for left-handed compounds). Each double helicate is built up from two left-handed or right-handed single-helical chains that are coupled up by eight-coordinated Ln^{III} centres, of which each single left-handed or right-handed single-helical chain is built up by L- (for left-handed) or D-tartaric acids (for right-handed) bridging six-coordinated molybdenum atoms (Fig. 2). A possible formation process of the double helices is depicted in Scheme 1. Each Mo^{VI} atom in all compounds is coordinated *via* two terminal oxygen atoms (Mo–O 1.684(7)–1.719(4) Å), two hydroxyl oxygen atoms (Mo–O 1.941(7)–1.968(10) Å) and two carboxylate oxygen atoms (Mo–O 2.199(11)–2.244(9) Å) from two tartaric acid ligands. The six-coordinated Mo atoms are linked up by L-tartaric acid (or D-tartaric acid) to form left-handed (or right-handed) single-helical chains, which are intertwined themselves with a period of 18.475(1)–18.744(1) Å. Such two helical chains are linked together in a couple by eight-coordinated Ln^{III} atoms through coordinating to two carboxylate oxygen atoms of two tartaric acids on the outside of the helices to form very interesting enantiopure left-handed (bridged by L-tartaric acids) or right-handed (bridged by D-tartaric acids) double helicates. The coordinated oxygen atoms around each Ln^{III} cation, which are in distorted eight-coordinated square-antiprismatic geometries, are six aqua ligands (Ln–O 2.315(8)–2.483(8) Å), two chelate carboxylate groups (Ln–O 2.265(6)–2.374(7) Å). It is very remarkable that such arrangements of the tartaric acids, Mo and Ln atoms generate very interesting channels along the 6_5 (for left handed double helicates) or the 6_1 (for right handed double helicate) axis (Fig. 3).

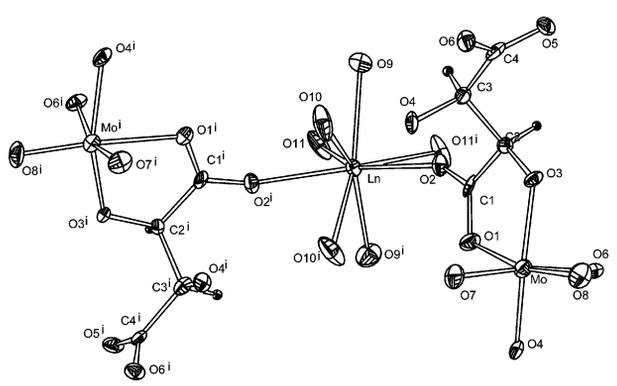

Fig. 1 A representative structure of the symmetry expanded structures (for L-tartaric acid) in **MoLn**, showing the coordination environments of Ln^{III} and Mo^{VI} atoms (symmetry code: i: $1-y, 1-x, 1/6-z$; 30% thermal ellipsoids probability).

Finally, it should also be pointed out, the crystallization H_2O molecules and/or NH_4^+ cations, which occupy the channels and among adjacent double helices, connect the double helices into three-dimensional frameworks *via* complex hydrogen bonds between the coordinated water molecules and the ligands (Fig. 4 and Table 4).

TGA and powder X-ray diffraction studies

The TGA for compounds **MoLn** (Ln = Sm, Gd, Dy, Ho) show continuous weight loss above about 30 °C and the curves have

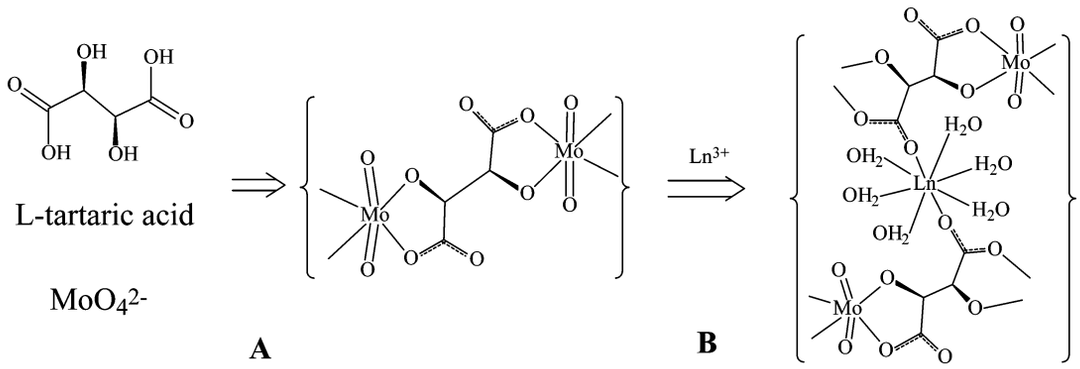

Scheme 1 Illustration showing (A) a left-handed helix being built up from very simple building blocks linked by L-tartaric acids and (B) how two such chains are linked by coordinated Ln^{III} ions assembled into a left-handed double helical complex.

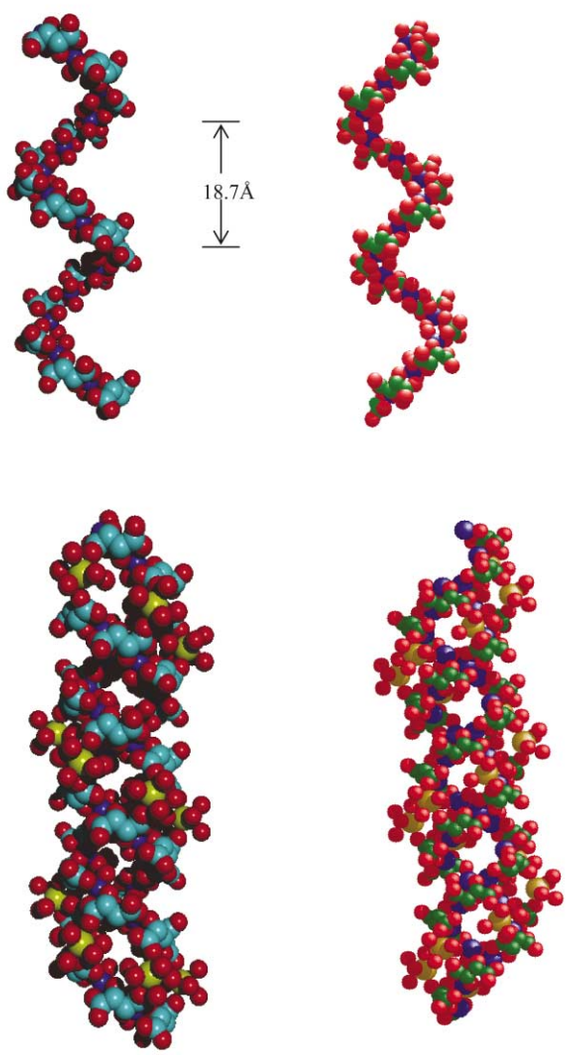

Fig. 2 Space-filling presentations: (top) one of the left-handed (left) and right-handed (right) helices; (bottom) the original left-handed (left) and right-handed (right) double helices (blue: Mo; purple or green: C; red or orange: O; yellow: Ln)

discernible inflection points at about 220 °C. The observed weight losses correspond to the loss of four crystallization water molecules and six aqua ligands per formula unit for each compound. Above 220 °C, the products begin to decompose. A sample of **MoGd** was heated at 70 °C under vacuum for 4 h and an XRPD was recorded for the heated sample. There is no sharp peak in the XRPD pattern. However, this material is easy rehydrated and reverted to the original compound after being immersed in water for twelve hours, or even exposed in moist

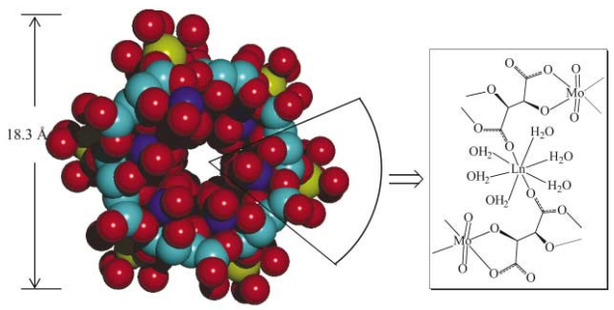

Fig. 3 Ball-and-scheme presentation of compounds **MoLn** (for left-handed double helicates) showing the channel viewed for each double helix down the 6_5 axis.

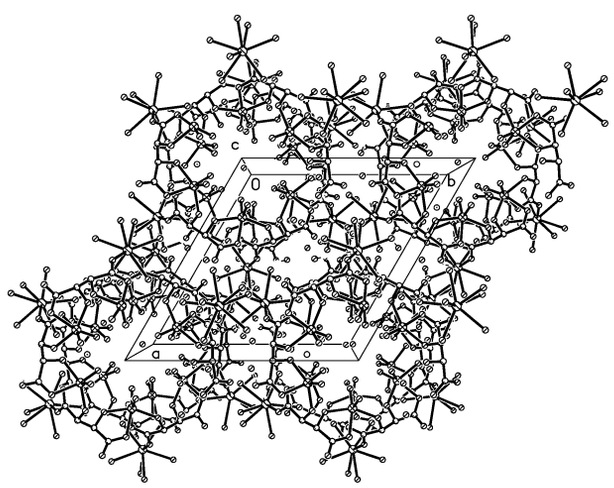

Fig. 4 The cell packing of **MoLn** showing the helix channels as well as the crystallization H_2O molecules and/or NH_4^+ cations down the *c* axis, which occupy the channels and between the spaces of adjacent double helices (hydrogen bonds are not shown for clarity).

air, as confirmed by comparing the XRPD patterns (Fig. 5). These results indicate that the crystallized H_2O and aqua ligands might play an important roles in the formation and stabilities of these compounds.

Electrical conductivities

The measurements of the temperature dependence of the electric conductivities for powder samples from ground crystals of **MoLn** (Ln = Gd, Ho, Eu, Y, Sm, Dy, Er and Yb) have also been carried out by using pressed small disks and the two probe technique. Although the samples used are in powder form and the influential factors on the measurement of absolute values of electric conductivities are more complicated than those for single crystals, the values should be reliable as their order of magnitudes are relative to the changing tendencies with the temperature. At 303 K, the electrical conductivities ($\times 10^{-6}$ S

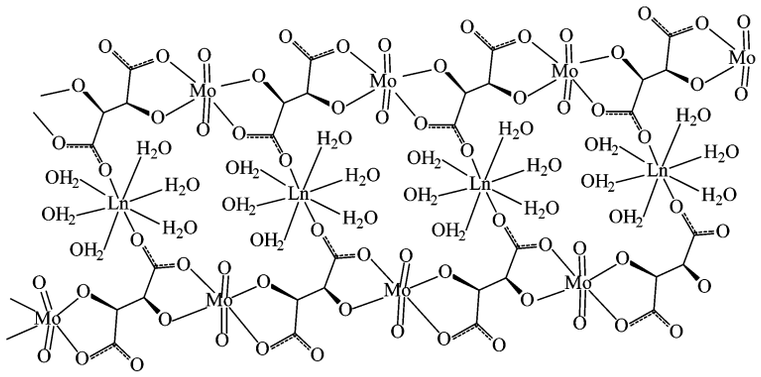

Scheme 2 Scheme representation of the double helicates (for left-handed).

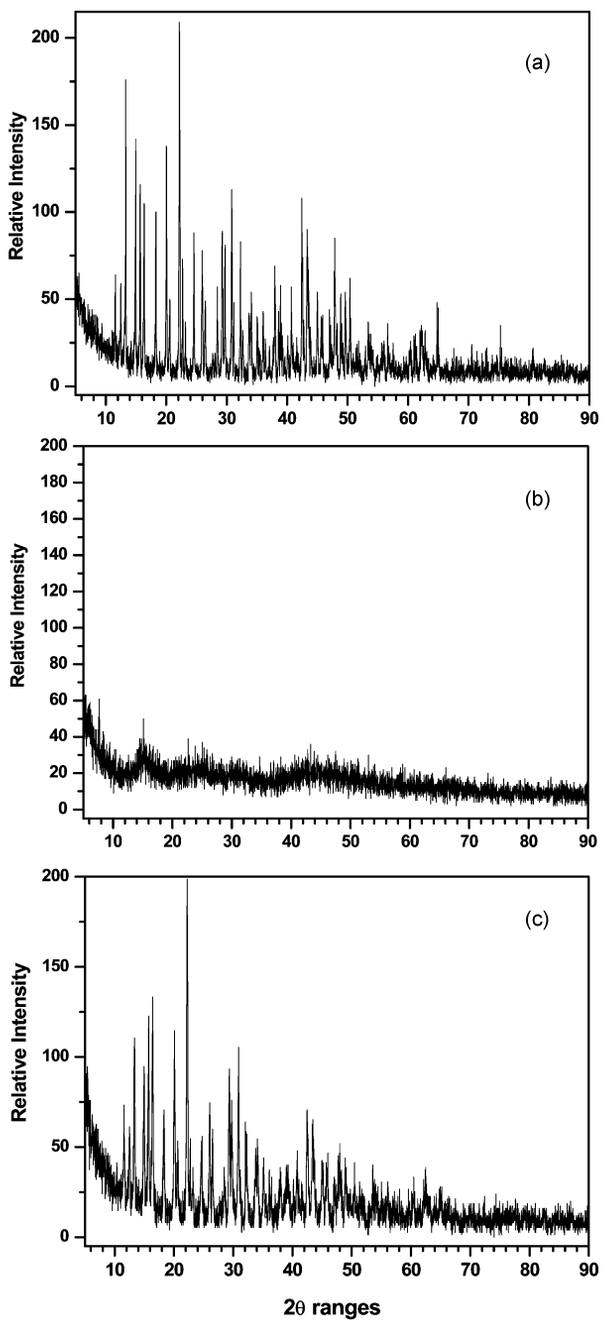

Fig. 5 Powder X-ray diffraction patterns before (top), after (middle) the removal of the water molecules and aqua ligands and for the sample re-immersed in water (bottom) for compound **MoGd**.

cm^{-1}) are 27.03 for Gd, 5.05 for Ho, 3.28 for Eu, 2.17 for Y, 1.48 for Sm, 0.96 for Dy, 0.80 for Er and 0.061 for Yb (and increase with temperature), indicating that these complexes are semiconductors.[21] As shown in Scheme 2, the main differences concerning these structures simply relate to the different lanthanide atoms. By comparison the conductivities of these compounds, the different conductivities at same temperature should be attributed to their different number of 4f electrons and radii of these lanthanide ions. After removal of the crystallized H_2O and aqua ligands, the electrical conductivities for the dry sample of **MoGd** are $>1.0 \times 10^{-9}$ S cm^{-1}, which suggests that it becomes an insulator and the conjugation system for transmission of electrons was destroyed. However, as aforementioned, it is very interesting that the electrical conductivities of the reverted sample are very similar to the original (Fig. 6).

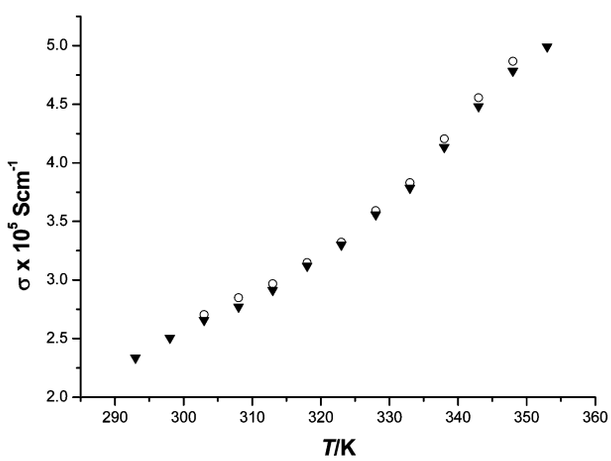

Fig. 6 Plot of the temperature dependence of electrical conductivities before the removal of the water molecules (○) and after the re-immersion of the evacuated sample in water (▼) for compound **MoGd**.

Magnetic properties

The powder magnetic susceptibilities for **MoLn** (Ln = Sm, Gd, Dy, Ho and Yb) have also been studied. Fig. 7 shows the magnetic behaviors for complexes **MoLn** (Ln = Gd, Dy, Ho and Yb) in the forms of $\chi_M T$ *vs.* T plots. The room temperature $\chi_M T$ values are 7.143, 8.781, 12.576 and 2.274 emu K mol^{-1} for per monomer Gd, Dy, Ho and Yb, respectively. The $\chi_M T$ values increase slightly to a maximum of 7.80 or 9.374 emu K mol^{-1} when the temperature was lowered to 30 or 26 K, and decreases to 6.97 or 6.56 emu K mol^{-1} at 4.2 K for the Gd or Dy complexes, while the $\chi_M T$ decreases slightly to a minimum of 6.85 or 1.78 emu K mol^{-1} when the temperature was lowered to 4.2 K for Ho or Yb complexes. As shown in Fig. 8, all data follow closely the Curie–Weiss law, with $C = 7.059$ emu K mol^{-1} and $\theta = 1.316$ K for **MoGd**, $C = 8.798(2)$ emu K mol^{-1} and $\theta = 0.310$ K for **MoDy**, $C = 12.642$ emu K mol^{-1} and $\theta = -2.191$ K for **MoHo**, $C = 2.306$ emu K mol^{-1} and $\theta = -2.437$ K for **MoYb**, indicating ferromagnetic interactions between the Gd^{III} or Dy^{III} cations and antiferromagnetic behaviors for Ho^{III} or Yb^{III}.

Since the ground state of gadolinium(III) ($^8S_{7/2}$) is orbitally nondegenerated and well separated from the excited state, Gd^{III}

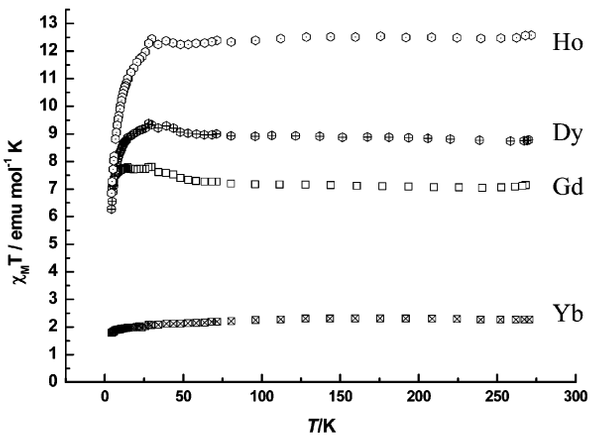

Fig. 7 Plots of the experimental temperature dependences of $\chi_M T$ for compounds **MoLn** (Ln = Gd, Dy, Ho, Yb).

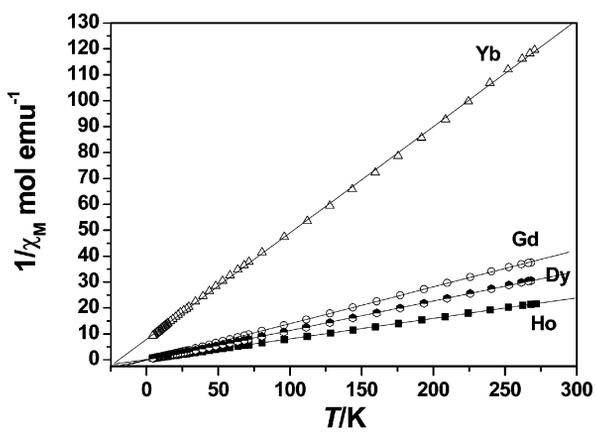

Fig. 8 The inverse susceptibilities with linear regressions based upon the Curie–Weiss law for **MoLn** (Ln = Gd, Dy, Ho, Yb).

shows a simple single ion magnetic properties. The profile of the curve indicates that the Gd–Gd interactions are ferromagnetic. The decrease of $\chi_M T$ below 30 K is attributed to weak intermolecular antiferromagnetic interactions. Therefore, to evaluate the magnetic interactions between the Gd ions, the experimental data were fitted to an isotropic chain model,[22] corrected by inter-chain coupling employing a molecular field to the susceptibilities. The least-squares fitting of the experimental data suggest the intra-chain Gd–Gd interactions are weakly ferromagnetic (J = 0.168 cm^{-1}), while weak antiferromagnetic interactions occur between adjacent chains (J' = 0.0335 cm^{-1}) with g = 1.90 (agreement factor $R = 2 \times 10^{-5}$). The EPR spectra of polycrystalline **1** give g = 1.90 at room temperature and 1.88 at 77 K, which are comparable to the results from magnetic measurements.

Conclusion

In conclusion, by using chiral organic ligands, L- or D-tartaric acid, a series of novel chiral left- or right-handed double helicates have been prepared and characterized, whose structures contain channels formed by double helical chains. To the best of our knowledge, these are the first extended enantiomerically pure hybrid materials, constructed from molybdenum and lanthanide atoms as well as chiral ligands. These compounds not only have fascinating architectures, but also exhibit interesting electric conductivities and magnetic properties. In addition, the frameworks can be regenerated after drying and re-immersion in water. They are rare examples of enantiomerically pure chemicals existing as isolated enantiomers in coordination chemistry, which suggest they may have potential applications as heterogeneous chiral catalysts or separation media that combine both shape selectivity and enantioselectivety.

Acknowledgements

This work was supported by the 973 Program of the MOST (001CB108906), the National Natural Science Foundation of China (90206040, 20073048), the Natural Science Foundation of Fujian Province (2002F015, 2002J006) and the Chinese Academy of Science.

References

1 S. I. Stupp and P. V. Braun, *Science*, 1997, **277**, 1242.
2 Z. Guo and P. J. Sadler, *Angew. Chem., Int. Ed.*, 1999, **38**, 1512.
3 D. Philp and J. F. Stoddart, *Angew. Chem., Int. Ed. Engl.*, 1996, **35**, 1154.
4 E. Rizzarelli and G. Vecchio, *Coord. Chem. Rev.*, 1999, **188**, 343.
5 D. J. Cram, *Angew. Chem., Int. Ed., Engl.*, 1988, **27**, 1009.
6 J. S. Lindsey, *New J. Chem.*, 1991, **15**, 153.
7 R. Breslow, *Science*, 1982, **218**, 532.
8 L. Liu and Q.-X. Guo, *J. Phys. Chem. B*, 1999, **103**, 3461.
9 P. D. Smith, D. A. Slizys, G. N. George and C. G. Young, *J. Am. Chem. Soc.*, 2000, **122**, 2946.
10 (*a*) C. Piguet, G. Bernardinelli and G. Hopfgartner, *Chem. Rev.*, 1997, **97**, 2005; (*b*) M. Albrecht, *Chem. Rev.*, 2001, **101**, 3457.
11 J.-M. Lehn, *Supramolecular Chemistry*, VCH, Weinheim, 1995.
12 (*a*) J. S. Seo, D. Whang, H. Lee, S. I. Jun, J. Oh, Y. J. Jeon and K. Kim, *Nature*, 2000, **404**, 982; (*b*) S. G. Telfer, B. Bocquet and A. F. Williams, *Inorg. Chem.*, 2001, **40**, 4818; (*c*) E. C. Constable, M. J. Hannon and D. A. Tocher, *Angew. Chem., Int. Ed. Engl.*, 1992, **31**, 230; (*d*) L. J. Childs, N. W. Alcock and M. J. Hannon, *Angew. Chem., Int. Ed.*, 2001, **40**, 1097; (*e*) J. Hamblin, A. Jackson, N. W. Alcock and M. J. Hannon, *J. Chem. Soc., Dalton Trans.*, 2002, 1635; (*f*) L. J. Charbonniere, A. F. Williams, C. Piguet, G. Bernardinelli and E. Rivara-Minten, *Chem. Eur. J.*, 1998, **4**, 485.
13 (*a*) V. Amendola, L. Fabbrizzi, C. Mangano, P. Pallavivini, E. Roboli and M. Zema, *Inorg. Chem.*, 2000, **39**, 5803; (*b*) L. Carlucci, G. Ciani, D. W. v. Gudenberg and D. M. Proserpio, *Inorg. Chem.*, 1997, **36**, 3812; (*c*) K. A. Hirsch, S. R. Wilson and J. S. Moore, *Chem. Commun.*, 1998, 13; (*d*) T. M. Garrett, *J. Chem. Soc., Chem. Commun.*, 1990, 557; (*e*) J.-M. Lehn, A. Riganlt, J. Siegel, J. Harrowfield, B. Chevrier and D. Moras, *Proc. Natl. Acad. Sci. USA*, 1987, **84**, 2565; (*f*) J.-M. Lehn and A. Riganlt, *Angew. Chem., Int. Ed. Engl.*, 1988, **27**, 1095; (*g*) O. Mamula, A. von. Zelewsky, T. Bark and G. Bernardinelli, *Angew. Chem., Int. Ed.*, 1999, **38**, 2945.
14 J. R. D. DeBord, Y.-J. Lu, C. J. Warren, R. C. Haushalter and J. Zubieta, *Chem. Commun.*, 1997, 1365.
15 (*a*) V. Soghomonian, Q. Chen, R. C. Haushalter, J. Zubieta and C. J. O'Connor, *Science*, 1993, **259**, 1596; (*b*) Z. Shi, S. Feng, S. Gao, L. Zhang, G. Yang and J. Hua, *Angew. Chem., Int. Ed.*, 2000, **39**, 2325.
16 C.-Z. Lu, C.-D. Wu, S.-F. Lu, J.-C. Liu, Q.-J. Wu, H.-H. Zhuang and J.-S. Huang, *Chem. Commun.*, 2002, 152.
17 C.-D. Wu, C.-Z. Lu, X. Lin, D.-M. Wu, S.-F. Lu, H.-H. Zhuang and J.-S. Huang, *Chem. Commun.*, 2003, 1284.
18 P. Pascal, *Ann. Chim. Phys.*, 1910, **19**, 5.
19 G. M. Sheldrick, SADABS; Siemens Analytical X-ray Instrument Division: Madison, WI, 1995.
20 G. M. Sheldrick, Universität Göttingen, Germany, 1997.
21 R. E. Newnham, *Structure–Property Relations*, Springer-Verlag, Berlin/Heidelberg/New York, 1975.
22 M. E. Fisher, *Am. J. Phys.*, 1964, **32**, 343.